Spin freezing and the ferromagnetic and reentrant spin-glass phases in a reentrant ferromagnet

T. Sato, T. Ando, and T. Ogawa
Department of Applied Physics and Physico-Informatics, Faculty of Science and Technology, Keio University, 3-14-1 Hiyoshi, Kohoku-ku, Yokohama-shi, Kanagawa, 223-8522 Japan

S. Morimoto and A. Ito*
Department of Physics, Faculty of Science, Ochanomizu University, Bunkyo-ku, Tokyo, 112-8610 Japan
(Received 8 September 2000; revised manuscript received 22 June 2001; published 22 October 2001)

The reentrant spin-glass (RSG) transition and the magnetic nature of the RSG and ferromagnetic (FM) phases of a standard reentrant ferromagnet (^{57}Fe-doped) NiMn were investigated using ac susceptibility and Mössbauer measurements. The spin-freezing temperature, at the observation time of the ac magnetic method, was determined by a peak in the in-phase component of nonlinear susceptibility. The distribution of the hyperfine field in the zero-field Mössbauer data consisted of two peaks in the FM phase but one antisymmetric peak in the RSG phase. The average hyperfine field rapidly increases so as to deviate from the Brillouin function below a certain temperature. The onset of deviation corresponds to spin freezing on the Mössbauer time scale. The two peaks in the hyperfine field in the FM phase were assigned to two kinds of spin groups having different relaxation times. The spin-freezing process can be explained based on the concept of ''melting of frustrated spins'' introduced by Saslow and Parker. The local magnetization, deduced based on the in-field Mössbauer data, was dependent on the applied field in the same manner as the magnetization in both the RSG and FM phases. This indicates that a spin-glass correlation coexists with ferromagnetic order in the RSG phase in a different way from the mean-field model for vector spin glasses. The application of a magnetic field induced one additional peak in the hyperfine field in the RSG phase. This implies that the long-range spin-glass order becomes unstable by applying a magnetic field in the RSG phase. Based on all the experimental results, we construct a comprehensive picture of a reentrant ferromagnet.

DOI: 10.1103/PhysRevB.64.184432 PACS number(s): 75.50.Lk, 75.30.Kz, 76.80.+y, 75.40.Gb

I. INTRODUCTION

In the last two decades, considerable attention has been paid to a class of random magnets, reentrant ferromagnets, which contain a majority of ferromagnetic couplings between the individual spins but also a sufficiently large number of antiferromagnetic couplings. As the temperature is lowered in this material, it undergoes a transition from a paramagnetic (PM) phase to a ferromagnetic (FM) phase, and as the temperature continues to decrease the material further undergoes a transition to a state known as a reentrant spin glass (RSG).[1] Reentrant ferromagnets have been understood on the basis of a mean-field model. In the Sherrington-Kirkpatrick mean-field model of the Ising spin system[2] and in the model of the Heisenberg spin system introduced by Gabay and Toulouse,[3] the ferromagnetic order parameter stays in the RSG state. This means that there is a low-temperature ''mixed'' state below a certain temperature in the ferromagnetic phase, in which the spin-glass behavior coexists with the long-range ferromagnetic order. In other words, ''true reentrance'' to the RSG phase without the long-range ferromagnetic order cannot occur in the mean-field models.

Recently, the Uppsala group studied the standard reentrant ferromagnet $(Fe_{0.20}Ni_{0.80})_{75}P_{16}B_6Al_3$, and obtained a result suggesting that the spin-glass relaxation time diverges at a finite transition temperature.[4,5] Based on this experimental observation, they claimed that an equilibrium reentrant spin-glass transition takes place from a ferromagnetic to a pure spin-glass phase. This was the first report to effectively characterize true reentrance in a reentrant ferromagnet based on the investigation of dynamic behavior. On the other hand, there are some reentrant systems in which the existence of the long-range ferromagnetic correlation has been found in the low-temperature phase.[6] In these systems, true reentrance to a pure spin-glass phase was questioned. In addition, the Uppsala group showed that the FM phase of a reentrant ferromagnet has a chaotic nature,[7] as expected in the conventional spin-glass phase.[8] This is in contrast to the robust nature of the regular ferromagnetic phase. This kind of feature, associated with the disorder and frustration accompanied by the appearance of the RSG phase, has not been sufficiently interpreted based on the mean-field model. Thus there remain some ambiguities related to the magnetic nature of both the RSG and FM phases in reentrant ferromagnets.

Observation of dynamic behavior, based on low-field susceptibility measurements at various observation times, is the most useful method of elucidating the nature of reentrant ferromagnets. In addition, complementary information can be obtained by a careful consideration of the complexity connected with magnetic inhomogeneity on various scales in space. In this work, we studied the RSG transition and the magnetic nature of RSG and FM phases of a typical reentrant ferromagnet based on the ac susceptibility and the Mössbauer spectra using comprehensive information about the dynamic nature and the spatial complexity of this magnet.

The binary system NiMn, with Mn concentrations from ~19 to 23.9% shows the typical behavior of reentrant ferromagnet.[9] In a reentrant sample, the ferromagnetic domain was directly observed in the low-temperature region by transmission electron microscopy.[10] The authors of Ref. 11

claimed that the RSG phase is a mixed state which exhibits spontaneous magnetization, as based on static magnetic measurements. In addition to a large number of magnetic measurements, small-angle neutron scattering (SANS),[12,13] inelastic neutron scattering[14] and neutron depolarization analysis[15,16] have also supported the existence of the long-range ferromagnetic correlation in the RSG phase. On the other hand, SANS measurements performed in a magnetic field showed that a magnetic structure, different from the ferromagnetic arrangement, is induced mainly in the transverse spin components.[13,16] In addition, we briefly reported that the Mössbauer spectrum of Fe-doped NiMn yields two peaks in the hyperfine field distribution.[17] Very recently, we found that both the RSG and FM phases of a reentrant ferromagnet Pt-doped NiMn show aging behavior, which was expected based on the droplet model,[18] and chaotic behavior through the relaxation of magnetization dependent on the waiting time and the temperature cycle.[19] Taken together, the experimental observations of the reentrant ferromagnet NiMn have suggested the following features.

(1) The RSG phase is a mixed state in which the long-range ferromagnetic correlation coexists with the spin-glass order, as expected from the mean-field picture.

(2) The aging effect and chaotic nature are observed even in the FM phase in addition to the RSG phase, although not expected from the mean-field picture.

(3) The spin structures of FM and RSG phases are nonuniform, and are sensitively modified by an applied magnetic field.

Therefore, it is interesting to comprehensively inspect the RSG transition and magnetic nature of the RSG and FM phases of NiMn in light of a detailed consideration of the resolution of time and the spatial scales of experimental methods. We believe that this yields some fruitful information that may help to solve the problem: ''Why is it difficult to systematically interpret the reentrant phenomena based on a theoretical viewpoint?''

In this work, we study the magnetic properties of the RSG and FM phases in a reentrant ferromagnet, ^{57}Fe-doped NiMn($Ni_{77}{}^{57}Fe_1Mn_{22}$), mainly using the ac susceptibility and Mössbauer techniques, which have rather different spatial resolutions and observation times. We first study spin-freezing behavior based on the ac susceptibility. Next we analyze the zero-field Mössbauer data as a function of temperature. The thermal evolution of the distribution of the hyperfine field is associated with a change in spin dynamics. This process is discussed using the concept of ''melting of frustrated spins'' introduced by Saslow and Parker.[20] Based on this, we have a clue toward understanding the magnetic nature of the ferromagnetic phase and the spin-freezing process. In addition, the in-field Mössbauer data are analyzed. This is suggestive of the following two phenomena: The long-range ferromagnetic correlation coexists with the long-range spin-glass order in the RSG phase in the different way from the mean-field picture, and the long-range spin-glass correlation becomes unstable in a magnetic field. The latter phenomenon is similar to the observed lack of a phase transition in a magnetic field in three-dimensional Ising spin-glasses.[21] Based on all the experimental results, a comprehensive picture of a reentrant ferromagnet will be constructed.

II. EXPERIMENT

The procedure for preparing $Ni_{77}{}^{57}Fe_1Mn_{22}$ was similar to that for preparing NiMn (Ref. 16): Ni, Mn, and ^{57}Fe were arc melted together under argon in the desired composition, and the ingot was homogenized for three days at 900 °C and then quenched in water. The sample, rolled to 0.02 mm in thickness, was used for the Mössbauer measurements. This sample had been used in our previous Mössbauer study.[17] A roll of the thin sheet, with $8\times12\times0.02\,\mathrm{mm}^3$, was used for the magnetic measurement.[22] The composition was determined by means of electron probe microanalysis, where the present detailed analysis resulted in a slightly lower Mn concentration than the nominal composition shown in Ref. 17. There was no gross inhomogeneity of the composition in the sample. In a previous study,[17] we roughly estimated the PM-FM transition temperature T_C to be ~150 K and the RSG transition temperature T_{RSG} to be ~50 K, although these temperatures will be precisely reevaluated in this paper. These transition temperatures are comparable to those of the reentrant system NiMn with the same Mn concentration.[9]

The ac susceptibility was measured at a frequency $\omega/2\pi = 210$ Hz by a Hartshorn-type mutual inductance bridge. The in-phase and out-of-phase components χ_0' and χ_0'' of the linear ac susceptibility can be separately measured by a lock-in amplifier. The longitudinal ac susceptibility was measured in a dc field applied parallel to the ac field using an air-core coil. In addition, the nonlinear susceptibility χ_2^t, was obtained by extracting the 3ω component from the ac magnetic response using the lock-in technique.[23]

Zero-field Mössbauer measurements were performed at temperatures above 4.6 K in the transmission arrangement using a conventional constant-acceleration spectrometer. In addition, the Mössbauer spectra were obtained in a magnetic field of up to 15 kOe, applied along the γ ray, at 4.6 and 78 K. An isomer shift of ~0.06 mm/sec and a zero quadrupole splitting were obtained from the spectra. We evaluated the hyperfine field distribution based on the method developed by Hesse and Rubartsch.[24]

III. RESULTS AND DISCUSSION

A. ac susceptibility

Figures 1(a) and 1(b) show the temperature-dependent ac susceptibilities, measured at $\omega/2\pi = 210$ Hz, for ac fields $h = 0.4$ and 0.2 Oe. In addition, a dc field for $H < 5$ Oe was superimposed. We will first focus on the magnetic data in the FM regime. The in-phase component χ_0', for $h = 0.2$ Oe and $H = 0$, shows a peak at $T \sim 130$ K, and is gradually suppressed as the temperature decreases. The peak position shifts to lower temperature as the field h increases from 0.2 to 0.4 Oe. The successive shift is found in the superimposed dc field. The out-of-phase component χ_0'', for $h = 0.2$ Oe and $H = 0$, shows a peak at ~140 K, which signals the PM-FM transition, and at temperatures below the peak position shows a decrease followed by a plateau region. This peak is

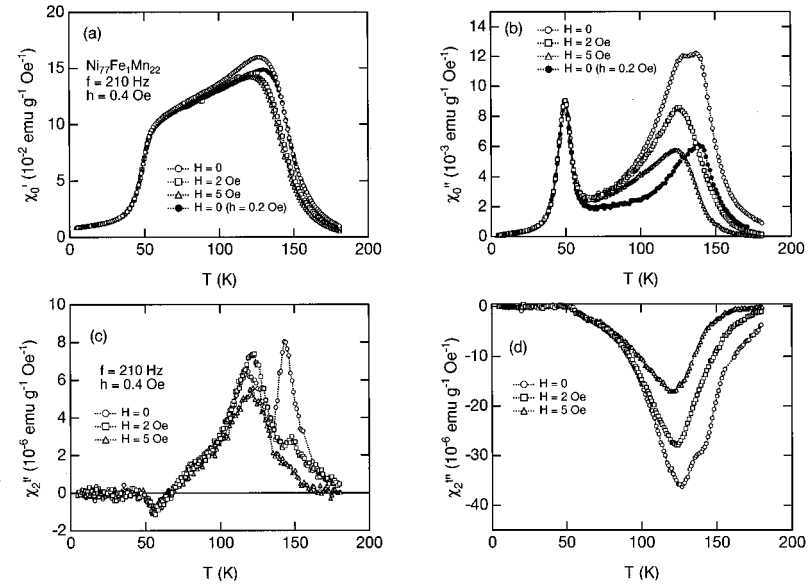

FIG. 1. In-phase component χ_0' (a) and out-of-phase component χ_0'' (b) of linear ac susceptibility of $Ni_{77}Fe_1Mn_{22}$ as a function of temperature, measured at a frequency of 210 Hz in the ac fields $h=0.2$ and 0.4 Oe and the superimposed dc fields $H=2$ and 5 Oe. The in-phase component $\chi_2^{t'}$ (c) and the out-of-phase component $\chi_2^{t''}$ (d) of the nonlinear ac susceptibility as a function of temperature are also represented, where the ac field $h=0.4$ was used.

significantly enhanced as the ac field increases from 0.2 to 0.4 Oe. In addition, a shoulder appears in χ_0'' at a temperature lower than the peak position for $h=0.4$ Oe. This shoulder successively changes to a broad peak in the data obtained in the superimposed dc field. The broad peak (or the shoulder) in χ_0'' appears at ~2.5 K higher than the corresponding peak temperature in χ_0'. The appearance of the peaks in χ_0' and χ_0'' can be explained based on the shape of the hysteresis loop, i.e., the peak corresponds to a temperature where the coercive field increases so that the hysteresis loop is traversed to reach the peak value of the ac field, since the magnetic susceptibility should attain a maximum when the coercive field is roughly equivalent to the applied field.[4]

Next we will focus on the low-temperature behavior associated with the RSG transition. The value of χ_0' is drastically suppressed below a certain temperature upon lowering the temperature in the ferromagnetic phase. In the lower temperature region, χ_0' is independent of the amplitudes of both h and H. The out-of-phase component shows a sharp peak at $T\sim 50$ K, below which all the data coalesce in a unique curve. The H independence of χ_0' and χ_0'' is a sign indicating that a material has entered into a spin-glass region in ordinary spin glasses.[21]

The nonlinear ac susceptibility was measured at $\omega/2\pi=210$ Hz and for ac fields $h=0.4$. The in-phase component of nonlinear ac susceptibility, $\chi_2^{t'}$, has the following characteristics: a sharp peak at a high temperature, a broad maximum in the ferromagnetic regime, and a small peak, with the opposite sign, at a low temperature below which $\chi_2^{t'}$ disappears independent of the amplitude of H [Fig. 1(c)]. The out-of-phase component, $\chi_2^{t''}$, for $H=0$ exhibits a shoulder at a temperature higher than the position of the broad maximum in the ferromagnetic region, corresponding to the PM-FM transitdion. Below ~50 K, $\chi_2^{t''}$ disappears independent of the amplitudes of H [Fig. 1(d)]. Based on the high-temperature peak in $\chi_2^{t'}$, $T_C=144$ K is precisely determined. In addition, we evaluate the spin-freezing temperature of 56.0 K based on the low-temperature peak in $\chi_2^{t'}$, below which $\chi_2^{t'}$ and $\chi_2^{t''}$ reach 0.

B. Zero-field Mössbauer measurements

Figure 2 shows the representative Mössbauer spectra measured in a zero field and the corresponding distribution of the hyperfine field $H_{\rm hf}$. The best fit spectrum is shown by a solid line in Fig. 2(a) using the area ratio of the absorption lines of 3:2:1:1:2:3, which corresponds to the random orientation of $\mathbf{H}_{\rm hf}$. As mentioned in our previous paper,[17] the distribution of $H_{\rm hf}$, $P(H_{\rm hf})$, except for the low-temperature data, can be approximately expressed by the following equation consisting of two kinds of Gaussians [Fig. 2(b)]:

$$P(H_{\rm hf})=A_i\exp\left[-\frac{(H_{\rm hf}-\langle H_{\rm hf}\rangle_i)^2}{2\Delta_i^2}\right]+A_j\exp\left[-\frac{(H_{\rm hf}-\langle H_{\rm hf}\rangle_j)^2}{2\Delta_j^2}\right], \quad (1)$$

where $\langle H_{\rm hf}\rangle_{i,j}$ and $\Delta_{i,j}$ are the average value and standard deviation of $H_{\rm hf}$ in each peak. Hereafter, these peaks will be referred to as $P_{\rm high}$ and $P_{\rm low}$. The low-temperature distribution of $H_{\rm hf}$, obtained below 50 K, consists of a single peak which is asymmetrically broadened towards the lower side of $H_{\rm hf}$.

Figure 3(a) shows the temperature dependence of the average value of $H_{\rm hf}$, where at temperatures higher than 50 K the values of $\langle H_{\rm hf}\rangle_{\rm high}$ and $\langle H_{\rm hf}\rangle_{\rm low}$, deduced from Eq. (1), are separately shown. The value of $\langle H_{\rm hf}\rangle_{\rm high}$, deduced at temperatures higher than 50 K, successively changes to $\langle H_{\rm hf}\rangle$ in the low-temperature region. Therefore, the thermal evolution of the hyperfine field can be discussed without making a distinction between both values. The average value of $H_{\rm hf}$ is compared with the Brillouin function ($S=\frac{1}{2}$ and $\frac{5}{2}$) using the Curie temperature $T_C=144$ K. The unambiguous

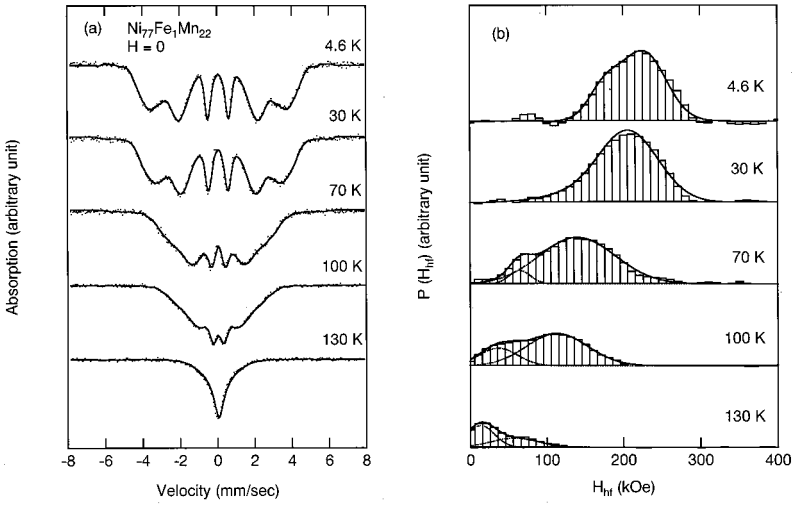

FIG. 2. Representative Mössbauer spectra of $Ni_{77}Fe_1Mn_{22}$ performed at a zero field (a) and the distribution $P(H_{\rm hf})$ of a hyperfine field (b).

deviation from the Brillouin function can be detected at temperatures below ~70 K.[25] This kind of deviation is similar to that observed for the other reentrant ferromagnets.[26] In addition, we can find that the behavior of $\langle H_{\rm hf}\rangle_{\rm low}$ also correlates with this deviation. Figure 3(b) shows the full width at half the maximum of the peak $\Delta H_{\rm hf}$. A maximum at $T\sim 60$ K is a noticeable observation in $\Delta H_{\rm hf}$ for $P_{\rm high}$. Figure 3(c) shows the normalized area of $P_{\rm low}$, $S_{\rm low}/(S_{\rm low}+S_{\rm high})$, as a function of temperature. This monotonically decreases as the temperature decreases, abruptly drops at temperatures below 70 K, and reaches 0 below 50 K. After all, all the values of $\langle H_{\rm hf}\rangle$, $\Delta H_{\rm hf}$, and $S_{\rm low}/(S_{\rm low}+S_{\rm high})$ show the singular behavior due to the spin-freezing at temperatures between 60 and 70 K. Thus the spin-freezing temperature of 60–70 K is evaluated at a typical observation time $t\sim 5\times 10^{-9}$ sec in Mössbauer measurement. This is higher than $T_f(t\sim 7.6\times 10^{-4}\ \text{sec})=56.0$ K, which was determined based on the ac susceptibility, because of the short observation time of Mössbauer measurement.[27]

C. In-field Mössbauer measurements

The Mössbauer data were obtained in magnetic fields at 4.6 and 78 K, on an increase in the applied field. Figure 4(a) shows the distribution of $H_{\rm hf}$ at 4.6 K at various values of the effective magnetic field $H_{\rm eff}$, where $H_{\rm eff}$ is given by correcting the applied field for the demagnetization field. In the analysis of $P(H_{\rm hf})$, the area ratio α of the (2,5) line, defined as the ratio $3{:}\alpha{:}1{:}1{:}\alpha{:}3$ for the lines of the sextet, was used as a free parameter in the fitting procedure. As mentioned in Sec. III C, we associate $P(H_{\rm hf})$ for $H=0$ with an asymmetric peak. This peak is slightly affected by the applied field, as shown in Fig. 4(a). It is worth noting that a similar kind of asymmetric distribution of $H_{\rm hf}$ was found in a strongly interacting magnetic nanoparticle system in a spin-freezing state at zero field.[28] The asymmetric peak, therefore, is a common feature observed in magnetic systems with a wide distribution of relaxation times. In a finite applied field, in addition, a peak appears on the lower-field side of the main peak. Therefore, the asymmetric main peak is attributed to the in-

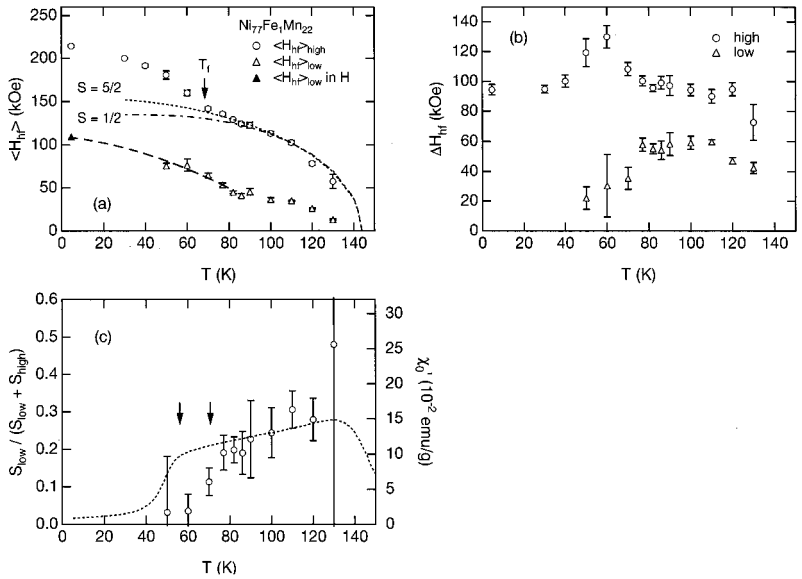

FIG. 3. The average value of $H_{\rm hf}$, obtained from the zero-field Mössbauer spectra, is shown in (a), where at temperatures higher than 50 K the values of $\langle H_{\rm hf}\rangle_{\rm high}$ and $\langle H_{\rm hf}\rangle_{\rm low}$ are deduced from Eq. (1). The Brillouin function ($S=1/2$ and 5/2) is shown in (a) in comparison with $\langle H_{\rm hf}\rangle_{\rm high}$. The dashed line shows that the in-field value of $\langle H_{\rm hf}\rangle_{\rm low}$ obtained at 4.6 K (closed triangle), is smoothly connected to the values of $\langle H_{\rm hf}\rangle_{\rm low}$ obtained in the ferromagnetic regime. The full width at half the maximum $\Delta H_{\rm hf}$ of peaks in $P(H_{\rm hf})$ (b) and the normalized area of the $P_{\rm low}$, $S_{\rm low}/(S_{\rm high}+S_{\rm low})$ (c) are shown as a function of temperature, where in-phase component χ_0' of the linear ac susceptibility is shown by a dotted curve in (c) for the sake of comparison. The freezing temperatures, evaluated based on the ac susceptibility and Mössbauer measurements, are shown by arrows in (c).

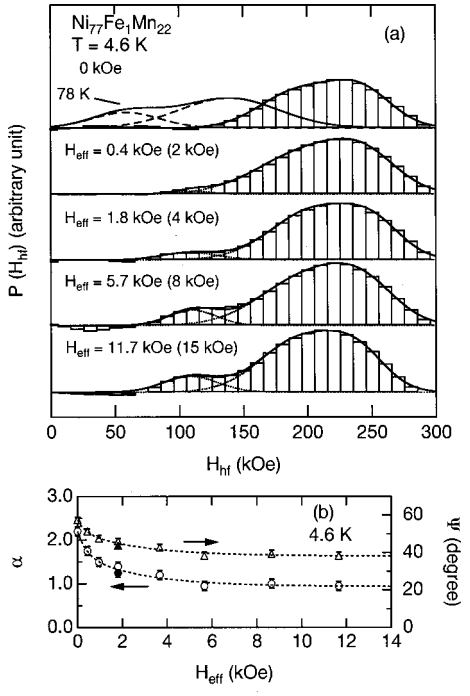

FIG. 4. A representative distribution of the hyperfine field, obtained from the in-field Mössbauer spectra measured at 4.6 K, is shown in (a), where the magnitude of the applied field is shown in parentheses in addition to the effective magnetic field $H_{\rm eff}$. The area ratio α and the angle Ψ are shown as functions of the applied field at 4.6 K (b), where the closed symbols show data obtained after the applied field decreases to 4 kOe from the highest field. The dotted line is provided as a guide.

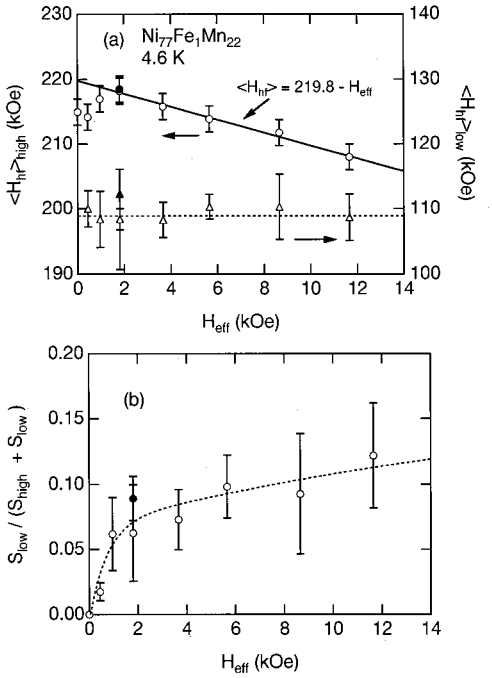

FIG. 5. Applied field dependence of $\langle H_{\rm hf}\rangle$ (a) and $S_{\rm low}/(S_{\rm high}+S_{\rm low})$ (b) obtained based on the Mössbauer spectra measured at 4.6 K, where the closed symbols show data obtained after the applied field decreases to 4 kOe from the highest field. The solid line in (a) shows the relation $\langle H_{\rm hf}\rangle_{\rm high}=219.8-H_{\rm eff}$. The dotted line is provided as a guide.

trinsic magnetic environment inherent in the low-temperature phase, and the resulting peak reflects an appearance of a different magnetic environment induced by the applied field. For 78 K, as mentioned above, there are two kinds of peaks in $P(H_{\rm hf})$ even at $H_{\rm eff}=0$ [the $P(H_{\rm hf})$ for $H_{\rm eff}=0$ is shown in Fig. 4(a)]. These peaks are insignificantly affected by the applied field. The area ratio α is associated with the angle Ψ, between the hyperfine field $\mathbf{H}_{\rm hf}$ and the direction of γ rays, by the relation

$$\alpha=\frac{4\sin^2\Psi}{2-\sin^2\Psi}. \tag{2}$$

The applied field dependence of α and Ψ in the RSG phase (4.6 K) are shown in Fig. 4(b). These values monotonically decrease as the magnetic field increases, but the comparatively large value of $\alpha\sim1$, corresponding to $\Psi\sim40°$, remains even at the highest magnetic field used in the present work.

In order to adequately describe the distribution of $H_{\rm hf}$, the applied field dependence of $\langle H_{\rm hf}\rangle$, and $S_{\rm low}/(S_{\rm high}+S_{\rm low})$ at 4.6 K, is shown in Fig. 5.[29] We will first focus on the values of $\langle H_{\rm hf}\rangle$. The applied field dependence of $\langle H_{\rm hf}\rangle_{\rm high}$ is linear with a gradient of -1; i.e., $\langle H_{\rm hf}\rangle_{\rm high}=219.8-H_{\rm eff}$ [the solid line in Fig. 5(a)], except for the low applied field region. This implies that the orientation of the hyperfine field is antiparallel to the magnetization. The value of $\langle H_{\rm hf}\rangle_{\rm low}$ is essentially independent of the applied field. This value is plotted in Fig. 3(a) using a closed triangle: it is consistently connected to $\langle H_{\rm hf}\rangle_{\rm low}$ in the ferromagnetic region, as shown by a dashed line. This feature strongly suggests that the appearances of $P_{\rm low}$ in both the FM and RSG phases share a common origin. The normalized area of $P_{\rm low}$, $S_{\rm low}/(S_{\rm high}+S_{\rm low})$, increases rapidly as the applied field increases and tends to become saturated at high fields [Fig. 5(b)]. Regarding the field dependence of $P(H_{\rm hf})$ obtained at 78 K, we cannot find any characteristic behavior.

D. Magnetic nature of the FM and RSG phases

We will now turn our attention to the appearance of two peaks of the hyperfine field, $P_{\rm high}$ and $P_{\rm low}$ in the ferromagnetic phase. One may suspect that this kind of multipeak profile is attributed to some accidentally induced chemical inhomogeneity. However, this idea is in contradiction with the single peak in the distribution of $H_{\rm hf}$ at low temperatures. The only possibility is that these peaks are assigned to two kinds of regions consisting of spins having different relaxation times. This is due to the peculiar distribution of relaxation time in the FM phase of the reentrant ferromagnet. This is in contrast to the regular ferromagnetic material, in which a single narrow peak appears in the hyperfine field distribution. From this viewpoint, the change in $S_{\rm low}/(S_{\rm low}+S_{\rm high})$ as the temperature approaches the RSG temperature must reflect the spin-freezing process in reentrant ferromagnets. Thus it is interesting to compare the thermal evolution of

$S_{low}/(S_{low}+S_{high})$ with the ac susceptibility which mirrors the relaxation time of the magnetic system. As shown in Fig. 3(c), the temperature dependence of $S_{low}/(S_{low}+S_{high})$ is similar to that of the in-phase component of ac susceptibility χ_0', although there is a difference between the temperatures at which $S_{low}/(S_{low}+S_{high})$ and χ_0' demonstrate this singular behavior. This kind of change in χ_0' is attributed to the slowing down of the spin relaxation as the system approaches the RSG transition from above. The decrease in the area of P_{low}, therefore, can be associated with the increase in the relaxation time. In other words, it suggests a shrinkage of the region consisting of spins with the shorter relaxation time. The considerable suppression of $S_{low}/(S_{low}+S_{high})$ occurs around the spin-freezing temperature ($\sim$70 K), i.e., the spin-freezing process is accompanied by the disappearance of spins with a shorter relaxation time, corresponding to P_{low}. Thus the maximum relaxation time diverges under the lack of P_{low} at the RSG transition temperature. This scenario may be reminiscent of the idea of the ''melting of frustrated spins,'' which was introduced as a mechanism to explain the reentrant transition in the two-dimensional (2D) model.[20] This mechanism is abridged as follows: above a temperature T_K, the frustrated spins are melted and then the ferromagnetic alignment of the other spins is stabilized in the FM phase; on lowering the temperature, the frustrated spins appear below T_K, and this induces a tilt of the ferromagnetic spins; as the temperature further decreases, the frustrated spins grow so as to be compared with the other spins, and the random spin configuration is completed. Apart from the inconsistency in the use of this 2D model, one may assign P_{low} and P_{high} to the spins around the melted spins and the ferromagnetically aligned spins. In this picture, in addition, the magnetic nature in the FM phase is strongly affected by the thermal evolution of frustrated spins. Such nonuniformity in the FM phase may induce spin-glass-like behavior such as the aging effect and the chaotic nature. On the other hand, the magnetic nature of the RSG phase is obviously inconsistent with the 2D model, as mentioned in the following paragraph.

Next, we discuss the field dependence of H_{hf} in comparison with the magnetization data in order to characterize the magnetic nature of the RSG phase. When a magnetic field $\mathbf{H}_{eff}$ is applied to the sample, the measured hyperfine field, $\mathbf{H}_{hf}$, directly obtained from the magnetic splitting in the Mössbauer spectrum, is given by the relation

$$\mathbf{H}_{hf}=\mathbf{H}_{hf}^{i}+\mathbf{H}_{eff}, \tag{3}$$

where $\mathbf{H}_{hf}^{i}$ is the intrinsic hyperfine field induced by the magnetic interaction when the relaxation time is longer than the observation time. As the orientation of the hyperfine field is antiparallel to the magnetization, the relation among $\mathbf{H}_{hf}$, $\mathbf{H}_{hf}^{i}$, and $\mathbf{H}_{eff}$ is expressed in the schematic drawing in the inset of Fig. 6. Based on the values of $\langle H_{hf}\rangle$, H_{eff}, and Ψ obtained up to this time, we can evaluate the average amplitude of the intrinsic hyperfine field $\langle H_{hf}^{i}\rangle$ and the angle Φ, between $\mathbf{H}_{hf}^{i}$ and the z axis, where the z axis is parallel to the applied field $\mathbf{H}_{eff}$. In a ferromagnetic ordering, H_{hf}^{i} is proportional to the local magnetization, and the measured magnetization M can be expressed as follows:

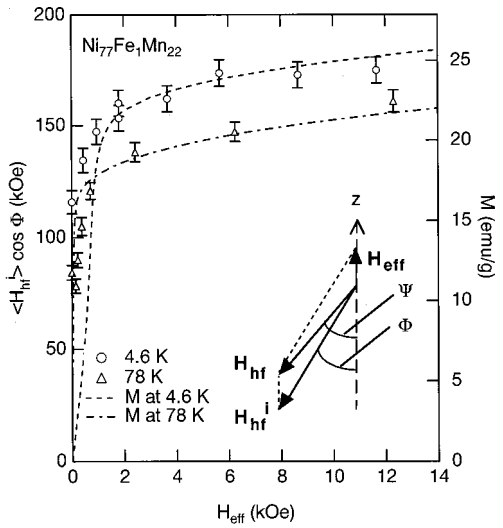

FIG. 6. The value of $\langle H_{hf}^{i}\rangle\cos\Phi$ is compared with the magnetization (expressed by dashed and dash-dotted lines) at 4.6 and 78 K (a), where H_{hf}^{i} and Φ are defined in the schematic drawing in (a).

$$M\propto\langle H_{hf}^{i}\rangle\cos\Phi=\langle H_{hf}\rangle\cos\Psi+H_{eff}. \tag{4}$$

As shown in Fig. 6, this relation is valid in both the FM (78 K) and RSG (4.6 K) phases.[30] This indicates that the hyperfine field in the RSG phase is governed by local magnetization in the same manner as in the FM phase, i.e., the spin order in the RSG phase, on a microscopic spatial scale, is qualitatively unchanged from the FM phase. This may not be expected from the mean-field model for the reentrant spin-glass phase in vector spin systems,[3] in which the additional hyperfine field, appearing at the RSG transition, originates from the transverse spin freezing. In addition, the present observation predicts that the local magnetization increases rapidly in the same manner as $\langle H_{hf}\rangle$ when a magnetic system approaches the spin-freezing temperature from above. This increase in local magnetization can be associated with the slowing down of spin fluctuation, i.e., a decrease in the longitudinal spin fluctuation. This is in accord with the following result of the neutron depolarization analysis:[16] the field integral, proportional to the amplitude of the local magnetic induction, rapidly increases as the temperature decreases from the FM phase to the RSG phase. In addition, this low-temperature spin dynamics may be consistent with the observation of the quasielastic scattering, coexisting with spin waves, in the inelastic neutron-scattering measurement of a reentrant NiMn below a temperature in the FM phase.[14]

Finally, we will discuss the nature of the RSG phase in a magnetic field. For this purpose, we will focus on the second peak, P_{low}. In the FM phase, this peak is abruptly smeared when the RSG temperature is approached from above in a zero applied field [Fig. 3(c)]. At 4.6 K, the same kind of peak is induced in $P(H_{hf})$ by applying a magnetic field, and the peak position is smoothly connected to that in the FM region [Fig. 3(a)]. As mentioned above, P_{low} in the FM phase is associated with spins with a larger amplitude of fluctuation: a

candidate for this is the melted spins. Thus the field-induced peak in the RSG phase should also be related to the same kind of spins. This implies that a spin fluctuation, faster than the observation time of the Mössbauer measurement, reappears in the low-temperature phase when a magnetic field is applied; i.e., there are regions where the freezing-spin is partially melted by the applied field. A possible explanation for this is that the ''melting of frustrated spins'' mechanism works even in the RSG phase when a magnetic field is applied. In this context, the long-range spin-glass ordering should become unstable because the melted spins stabilize the ferromagnetic alignment of spins. This situation is similar to the observed lack of a spin-glass transition in the ordinary 3D Ising-type spin glass $Fe_{0.5}Mn_{0.5}TiO_3$ in a magnetic field,[21] which was predicted by the droplet model.[8,18] In addition, the corresponding regions may be spatially ordered so as to agree with the in-field SANS data,[9,16] suggesting that a magnetic correlation, different from the ferromagnetic arrangement, appears in the RSG phase.

IV. CONCLUSION

The following picture of the spin-freezing process and the intrinsic nature of the RSG and FM phases of a reentrant ferromagnet was constructed via careful observation of the features dependent on the observation time and spatial resolution of the experimental apparatuses.

(1) In the FM phase, there are two kinds of regions consisting of spins with different relaxation times: these are assigned to spins around the melted frustrated spins with a shorter relaxation time and ferromagnetically aligned spins with a longer relaxation time.

(2) On lowering the temperature, a spin-glass correlation develops at the expense of spins with faster dynamics and then diverges at the RSG transition temperature. Such a nonuniformity in the FM phase, related to the behavior of frustrated spins, can induce a spin-glass-like behavior such as the aging effect and chaotic nature.

(3) In the RSG phase, a long-range ferromagnetic correlation coexists with the spin-glass order, but in a manner different from that of the mean-field model.

(4) When a magnetic field is applied in the RSG phase, the long-range spin-glass order becomes unstable through the ''melting of frustrated spins'' mechanism which originally works in the FM phase.

Obviously, the present picture, constructed so as to consistently explain a variety of aspects dependent on the experimental conditions, emphasizes the importance of precisely interpreting the nonuniformity which is observed in various situations. A comprehensive theoretical approach is certainly required to solve the reentrant problems.

ACKNOWLEDGMENTS

One of the authors (T.S.) would like to thank Professor Per Nordblad of Uppsala University (Sweden) for many stimulating discussions. Financial support from a Grant-in-Aid for Scientific Research from the Ministry of Education, Science, Sports, and Culture of Japan, from the Seki Foundation for the Promotion of Science and Technology and from the Izumi Science and Technology Foundation are gratefully acknowledged.

*Present address: Muon Science Laboratory RIKEN, 2-1 Hirosawa, Wako-shi, Saitama 351-0106, Japan.

[1] See, e.g., K. Binder and A. P. Young, Rev. Mod. Phys. **58**, 801 (1986); K. H. Fischer and J. Hertz, *Spin-Glasses* (Cambridge University Press, Cambridge, 1991); J. A. Mydosh, *Spin-Glasses* (Taylor & Francis, London, 1993).

[2] D. Sherrington and S. Kirkpatrick, Phys. Rev. Lett. **32**, 1782 (1975).

[3] M. Gabay and G. Toulouse, Phys. Rev. Lett. **47**, 201 (1981).

[4] K. Jonason, J. Mattsson, and P. Nordblad, Phys. Rev. B **53**, 6507 (1996).

[5] K. Jonason and P. Nordblad, J. Magn. Magn. Mater. **177–181**, 95 (1998).

[6] I. Mirebeau, S. Itoh, S. Mitsuda, T. Watanabe, Y. Endoh, M. Hennion, and R. Papoular, Phys. Rev. B **41**, 11 405 (1990).

[7] K. Jonason, J. Mattson, and P. Nordblad, Phys. Rev. Lett. **77**, 2562 (1996).

[8] A. J. Bray and M. A. Moore, Phys. Rev. Lett. **58**, 57 (1987).

[9] W. Abdul-Razzaq and J. S. Kouvel, Phys. Rev. B **35**, 1764 (1987).

[10] S. Senoussi, S. Hadjoudj, and R. Fourmeaux, Phys. Rev. Lett. **61**, 1013 (1988).

[11] J. S. Kouvel, W. Abdul-Razzaq, and Kh. Ziq, Phys. Rev. B **35**, 1768 (1987).

[12] M. Hennion, I. Mirubeau, F. Hippert, B. Hennion, and J. Bigot, J. Magn. Magn. Mater. **54–57**, 121 (1986); M. Hennion, I. Mirebeau, B. Hennion, S. Lequien, and F. Hippert, Europhys. Lett. **2**, 393 (1986); M. Hennion, B. Hennion, I. Mirebeau, S. Lequien, and F. Hippert, J. Appl. Phys. **63**, 4071 (1988); I. Mirebeau, M. Hennion, S. Lequien, and F. Hippert, *ibid.* **63**, 4077 (1988).

[13] S. Lequien, I. Mirebeau, M. Hennion, B. Hennion, F. Hippert, and A. P. Murani, Phys. Rev. B **35**, 7279 (1987).

[14] B. Hennion, M. Hennion, H. F. Hippert, and A. P. Murani, Phys. Rev. B **28**, 5365 (1983); J. Appl. Phys. **55**, 1694 (1984); J. Phys. F: Met. Phys. **14**, 489 (1984).

[15] I. Mirebeau, S. Itoh, S. Mitsuda, T. Watanabe, Y. Endoh, M. Hennion, and P. Calmettes, Phys. Rev. B **44**, 5120 (1991).

[16] T. Sato, T. Ando, T. Watanabe, S. Itoh, and Y. Endoh, J. Magn. Magn. Mater. **104–107**, 1625 (1992); T. Sato, T. Ando, T. Watanabe, S. Itoh, Y. Endoh, and M. Furusaka, Phys. Rev. B **48**, 6074 (1993).

[17] T. Sato, T. Ando, T. Oku, S. Morimoto, and A. Ito, J. Magn. Magn. Mater. **140–144**, 1781 (1995).

[18] D. S. Fisher and D. A. Huse, Phys. Rev. Lett. **56**, 1601 (1986).

[19] T. Sato and P. Nordblad, J. Magn. Magn. Mater. **226-300**, 1326 (2001).

[20] W. M. Saslow and G. N. Parker, Phys. Rev. Lett. **56**, 1074 (1986).

[21] J. Mattsson, T. Jonsson, P. Nordblad, H. Aruga Katori, and A. Ito, Phys. Rev. Lett. **74**, 4305 (1995).

[22] The demagnetizing factor $D \sim 0.2$ g Oe/emu, in $H_d = DM$ (H_d is the demagnetization field), is calculated for this sample, if the magnetic field is applied along the sheet plane. However, we evaluated the one order larger value of D in the present magnetic

measurement due to the incomplete arrangement between the sample and the magnetic field.

[23] T. Ando, E. Ohta, and T. Sato, J. Magn. Magn. Mater. **163**, 277 (1996).

[24] J. Hesse and A. Rubartsch, J. Phys. E **7**, 5 (1974).

[25] It is not easy to find the onset of an additional increase in the hyperfine field in excess of the value extrapolated from higher temperatures, because the temperature-dependent magnetization in the FM phase cannot be given by a conventional theoretical expression. We note that a previous experimental neutron study of $Ni_{80}Mn_{20}$ showed the Ni moments of $0.30\mu_B$/Ni and a Mn moment of $1.1\mu_B$/Mn. In addition, the Ni moment has an itinerant electron nature, while the Mn moment has a localized electron character [see J. W. Cable, R. M. Nicklow, and Y. Tsunoda, Phys. Rev. B **36**, 5311 (1987)].

[26] See, e.g., J. Lauer and W. Keune, Phys. Rev. Lett. **48**, 1850 (1982).

[27] Provided that these spin freezing temperatures are tentatively analyzed based on an expression of the critical slowing down,

$$\frac{t}{t_0}=\left(\frac{T_f(t)-T_{\mathrm{RSG}}}{T_{\mathrm{RSG}}}\right)^{-z\nu},$$

using $T_f(5\times10^{-9}\ \mathrm{sec})\sim65$ K, we evaluate $T_{\mathrm{RSG}}=54.2$ K and $z\nu=6.7$, assuming a microscopic spin flipping time t_0 of 10^{-13} sec. This evaluated value of $z\nu$ is comparable to what has been found in a reentrant ferromagnet $(Fe_{0.20}Ni_{0.80})_{75}P_{16}B_6Al_3$ ($z\nu=7.9$) (Ref. 4) and ordinary spin-glasses.

[28] Mikkel F. Hansen, Christian Bender Koch, and Steen Mørup, Phys. Rev. B **62**, 1124 (2000).

[29] The closed circle shows a datum obtained after the applied field decreases to 4 kOe from the highest field. Within the limit of experimental accuracy, reversible behavior does exist in the field dependence.

[30] In the FM region, $\langle H_{\mathrm{hf}}^i\rangle$ is approximately calculated based on $\langle H_{\mathrm{hf}}\rangle_{\mathrm{high}}$ because the magnetization is intrinsically related to the main distribution of the hyperfine field.